Induced Circularly Polarized Luminescence for Revealing DNA Binding with Fluorescent Dyes

Marcin Górecki, Francesco Zinna, Tarita Biver and Lorenzo Di Bari[*]

Dipartimento di Chimica e Chimica Industriale, Università di Pisa, via G. Moruzzi 13, 56124 Pisa, Italy
Email: lorenzo.dibari@unipi.it

Abstract

To the best of our knowledge this is the first report on the application of induced circularly polarized luminescence (CPL) for sensing the binding of fluorescent dyes to double stranded DNA. Using Thiazole Orange (TO) and 4',6-diamidino-2-phenylindole (DAPI) as models, we show utility and limitations of CPL in DNA binding studies. The results obtained indicate that CPL can be used as a new chiroptical tool for this purpose, however, special attention while recording CPL data must be used, in order to exclude measurement artefacts caused by linear polarization components.

Graphical abstract

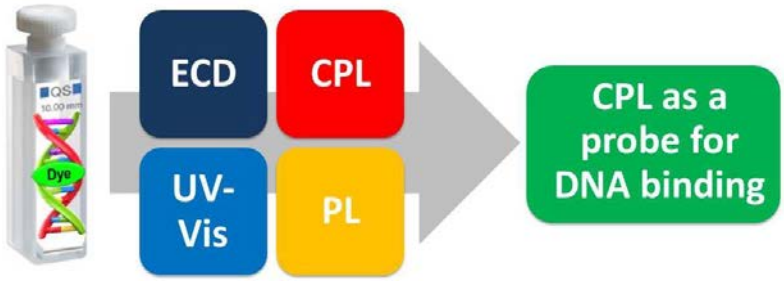

Keywords

Chiroptical methods, CPL, Electronic Circular Dichroism (ECD), DNA, Thiazole Orange (TO), 4',6-diamidino-2-phenylindole (DAPI)

Introduction

Interaction of small organic molecules like drugs, pollutants or stains with biomacromolecules has been targeted for decades by means of chiroptical spectroscopy. In the field of drug-carrier protein binding, Carlo Bertucci's contribution to the progress in the use and interpretation of induced circular dichroism (ICD) has been of prime importance.[1-4] Following this inspiration, and moved by our recent interest in circularly polarized luminescence (CPL), we decided to study the induction of CPL of fluorescent dyes upon their binding to DNA.

Circularly polarized luminescence (CPL) is the differential emission of left- *versus* right circularly polarized light in chiral non racemic molecules. It can be considered the emission counterpart of electronic circular dichroism (ECD), which takes place in absorption,[5,6] and the two techniques constitute a complementary set of chiroptical tools for probing excited and ground state structures of chiral entities. Recently CPL spectroscopy has found many new intriguing applications in different fields of pure and applied chemistry, such as chirality sensing of biomolecules,[7,8] such as amino acids,[9,10] sugars[11] and proteinaceous matrices,[12] chiroptical switching[13,14] or manufacturing new type of optoelectronic devices.[15-17] Furthermore, CPL and induced CPL has been efficiently utilized also for studying various bio-systems, including nicotinamide adenine dinucleotide,[18] oligonucleotide,[19] proteins,[20,21] insulin amyloid fibrils,[22] RNA,[23] chlorophyll[24] or chloroplasts.[25] This blossoming of CPL spectroscopy, followed and supported by the progress in instrumentation[26,27] and calculations[22,28-30] opens up new pathways to study chiral fluorescence systems and materials, but also lends itself to finding new challenges.

We decided to apply for the first time this technique to the interactions between calf thymus DNA (B-type double helix) and two different fluorescent dyes, *i.e.* Thiazole Orange (TO) and 4',6-diamidino-2-phenylindole (DAPI) (Fig. 1), which are commonly used to stain DNA. TO is a well-known fluorescent stain of the cyanine family that intercalates between DNA base-pairs,[31] whereas DAPI shows more complex behaviour but mainly yields groove-bound DNA complexes[31-33] and is used as minor-groove binding probe.[34,35] By using our protocol for recording CPL data,[12,30] we will show also some limitations of this technique and discuss the main origin of the artefacts standing behind. In addition, induced ECD (ICD) as a complementary spectroscopy to CPL will be also investigated for monitoring DNA-dye binding process.

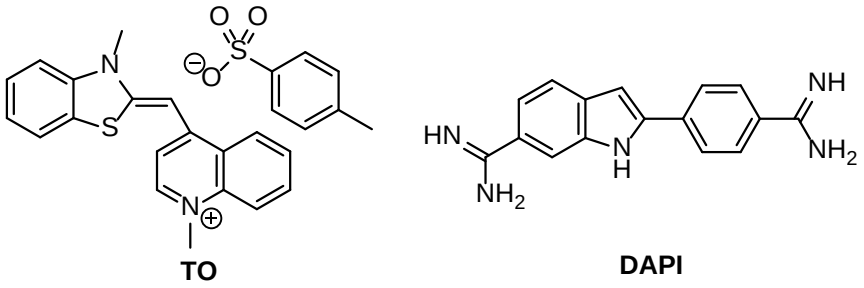

Fig. 1 Structure of Thiazole Orange (TO) and 4',6-diamidino-2-phenylindole (DAPI).

Materials and methods

Thiazole Orange (TO mono-cation, p-toluenesulfonate as counterion) was purchased from AnaSpec Inc. (ultrapure grade), whereas DAPI (4',6-diamidino-2-phenylindole·2HCl) was purchased from Merck. Stock solutions of TO and DAPI were prepared by dissolving appropriate amounts of the salts in DMSO (Sigma) to $C_{dye}= 1 \times 10^{-2}$ M. This stock solution was kept in the dark at 4 °C. Samples used for analysis were directly prepared in a cuvette with such a dilution of the stock in the working buffer (0.1 M NaCl and 0.01 M sodium cacodylate (NaCac) buffer, pH = 7.0) that the final content of DMSO is negligible. Calf thymus DNA (DNA) was the highly polymerised lyophilised sodium salt form (Sigma). It was sonicated to reduce the polynucleotide length (to *ca.* 500 base pairs) according to a known procedure.[36] DNA/TO and DNA/DAPI systems were prepared according respectively to Refs.[31,37]. The titrations were carried out at room temperature by adding increasing amounts of DNA directly to the cell containing the dye solution. The additions

were made by using a Hamilton syringe. For all solutions water was the ultra-pure grade from a Sartorius apparatus (18.2 MΩ cm at 25 °C).

Electronic circular dichroism (ECD)

The experimental ECD and UV-Vis spectra were recorded on a Jasco J-715 spectrometer at room temperature in a quartz cell with a path length of 1 or 2 cm. All measurements were carried out using a scanning speed of 100 nm min^{-1}, a step size of 0.2 nm, a bandwidth of 2 nm, a response time of 1 s, and an accumulation of 4 scans. The DNA/TO spectra were background-corrected using spectrum of the buffer recorded under the same conditions, while, because of some spectral overlap, DNA/DAPI spectra were background-corrected using the spectrum of DNA alone in buffer at the concentrations recorded under the same conditions.

Circularly polarized luminescence (CPL)

All CPL and fluorescence (PL) measurements were recorded using our home-built CPL spectrofluoropolarimeter described in Ref.[30]. TO/DNA samples were irradiated by a LED source (λ_{exc} = 470 nm) using a 90° geometry, as described previously[30]. A linear polarizing filter aligned with the optical axis of the detection apparatus was inserted between source and sample, to prevent photoselection artefacts. Removing this filter, however does not lead to major changes in the observed CPL signals.

DAPI samples were irradiated with a fluorescent UV lamp (λ_{exc} = 365 nm) using different 90° geometries: lamp to the side or on top of the sample, various lamp orientations.

All the spectra were carried out using a scanning speed of 60 nm/min, an emission slit width of *ca*. 10 nm, an integration time of 4 sec; each spectrum is the average of 4 accumulations.

Nuclear Magnetic Resonance (NMR)

NMR experiments were run on a Varian/Agilent INOVA 600 instrument operating at 14.1 T with a 5-mm triple resonance probe equipped with z-gradients. The experiments were run by adding directly 1μL of *tert*-BuOH as internal standard for quantitation of the ^1H integrals to samples consisting of 400 μL of DAPI dissolved in D_2O (8.5 mM) or CD_3OD (6.4 mM). In the spectra we used the integrals of non-overlapping DAPI signals, and the *tert*-buthyl resonance of the alcohol, all of them normalized for the number of resonating protons.

Results and Discussion

DNA/TO system

TO (**Fig. 1**, left) is a well known DNA-marker since it is strongly fluorescent upon complexation with DNA, and completely quenched in its free form in water.[38] These properties make TO an useful probe for revealing DNA and possibly also for studying various DNA conformations.[31,39-44] TO is achiral and for this reason its chiroptical spectra are vanishing. On the other hand, TO has electronic transitions much shifted to the red compared to DNA. These are ideal conditions to use the ICD to reveal the binding of dyes to DNA, as it is well established in the literature.[45-49] In order to find the best conditions for DNA/TO interaction, we first conducted ECD/absorption titration experiments, and then we recorded CPL spectra for selected mixture to highlight specific solution equilibria.

Figure 2 immediately reveals TO binding to DNA in the form of ICD signals in correspondence to the broad absorption band of TO around 500 nm: we must remember that the ICD signal can be generated only by the DNA/TO complex, because TO is achiral (black curve, DNA/TO=0:1), while DNA has no absorption in the visible. In the course of titration, a

sequence of a positive and a negative bands are found in the range 425-550 nm whose total and also relative magnitudes strongly depend on the DNA/TO mole ratio.

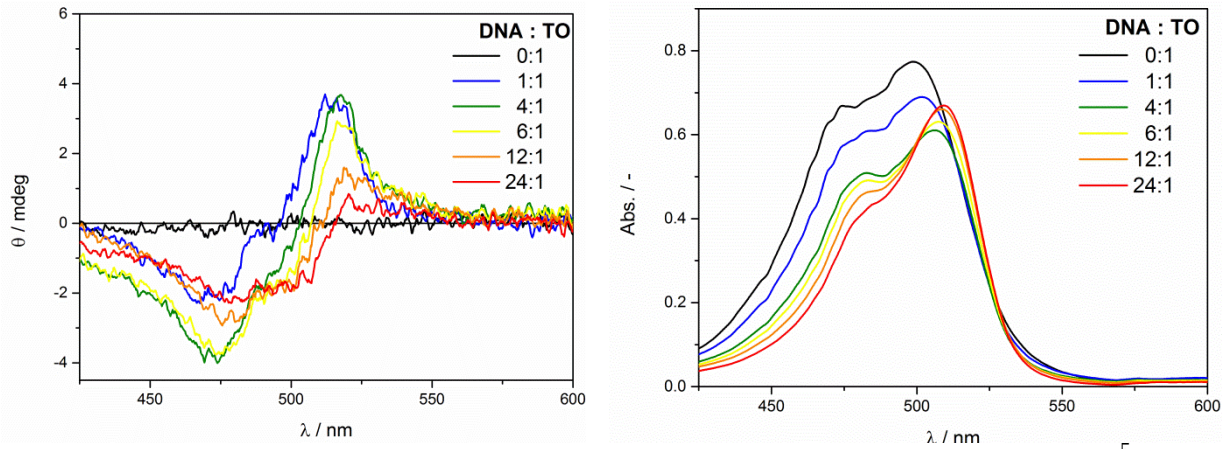

Fig. 2 ICD (left) and absorption (right) spectra of DNA/TO system (C_{TO} = 1.0 × 10^{-5} M) in 0.1 M NaCl and 0.01 M NaCac buffer (pH = 7.0) measured in the 2 cm path length cell.

Examining the changes of ICD spectra (Fig. 2, left) upon increasing the concentration of DNA, we can observe that there is no isodichroic point, owing to the fact that the relative intensities of the two main ICD bands change differently upon DNA addition: the positive band centred at *ca.* 510 nm systematically decreases from +4 mdeg (blue curve, DNA/TO=1:1) to almost disappear (+1 mdeg, red curve, DNA/TO=24:1) on increasing DNA, while the negative band at *ca.* 475 nm initially increases (absolute value) upon addition of DNA from –2 (DNA/TO=1:1) to –4 mdeg (DNA/TO=4:1) and then decreases to –2 mdeg (DNA/TO=24:1). Moreover, the positions of both positive and negative bands shift to the red by *ca.* 10 nm upon addition of DNA.

Similarly, in the absorption spectrum (Fig. 2, right), we first notice the absence of isosbestic point and the general change of spectral shape during the course of the titration. The relative ratio of the two bands changes from an approximate 1:0.9 to a 1:0.6. At the same time, like in the ECD spectra, one can observe that the position of the lowest energy band is 10 nm red-shifted with respect to the absorption spectrum of TO without DNA (black curve, DNA/TO=0:1). These observations are in line with previous work[31] where the presence of this dynamic equilibrium were reported by absorbance and fluorescence titrations.[50]

It was reported before, that at low DNA concentration TO may self-aggregate,[51] because the positively charged dye tends to concentrate in proximity of the negatively charged DNA.[31,48,52] As a first interpretation of the above chiroptical data, we can hypothesize that the DNA-bound TO aggregates may be responsible of the bisignate aspect of the ECD spectrum of Figure 2 during the first steps of the titration, which may be ascribed to intermolecular exciton coupling of the main electronic transition of TO. Indeed, there is a good match between the absorption λ_{max} and the ECD crossover, which is a typical signature of degenerate exciton coupling. Alternatively, it is also known that in free form TO has a certain degree of internal twist, leading to non-planar chiral conformations of the individual molecule, which was held responsible for the absence of fluorescence of the dye before DNA binding.[51] Interaction with DNA may induce the preference of a definite sense of twist, and this may constitute an alternative explanation of the observed ECD spectrum. At higher DNA concentration, however, a deep dye intercalation occurs,[53] and the broad negative band at about 490 nm may be allied to the coupling of the dye transitions with the neighbouring DNA bases. The redshift observed both in ECD and in the absorption spectrum may be the effect of

the different environment polarity from water to intercalation into nucleotide dyads and to planarization of the dye.[51]

Following these observations, we decided to collect the CPL data in the two limiting situations: one at low and one at high DNA:TO mole ratios (Fig. 3) and check the utility and sensitivity of CPL spectroscopy for sensing DNA with fluorescent dyes.

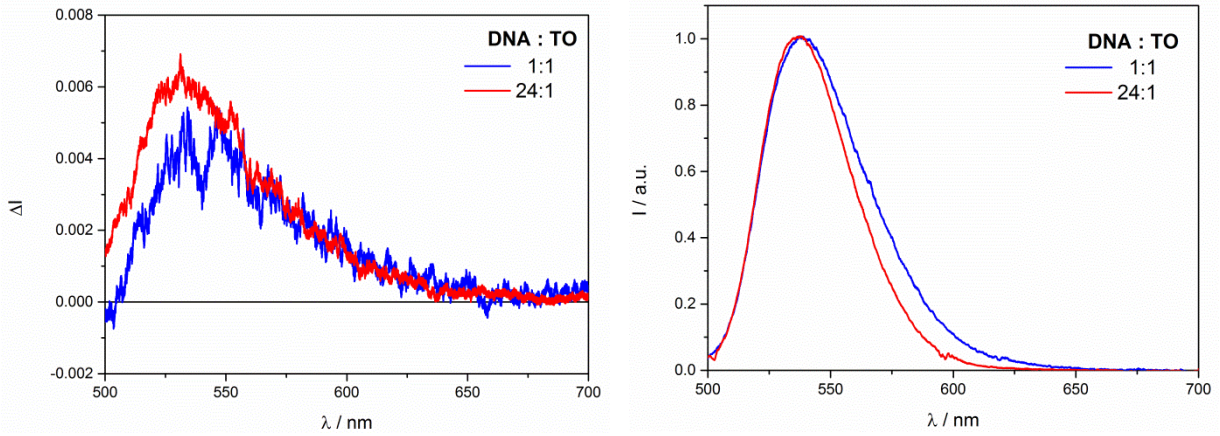

Fig. 3 Induced CPL (left) and normalized PL (right) spectra of DNA/TO system (C_{TO} = 1.0 × 10^{-5} M) in 0.1 M NaCl and 0.01 M NaCac buffer (pH 7.0) measured in the 1 cm path length cell.

The CPL spectra (Fig. 3, left) retrace the photoluminescence (PL) spectra (Fig. 3, right), showing a positive CPL band with a maximum in the range 530-540 nm. In contrast to ICD and absorption spectra, there is no shift of the CPL band with respect to the fluorescence band. The intensity of the CPL signal relative to total fluorescence (g_{lum}) remains essentially constant in both situations (DNA/TO=1:1 and DNA/TO=24:1), with a $g_{lum} \approx 5 \times 10^{-3}$ (the small differences are not deemed significant). It should be observed that in the latter situation TO appears much more emissive, which is well reflected in the improved signal-to-noise in the CPL spectrum compared to the low DNA concentration.

Based on Fig.s 2 and 3 (or Fig. S1, for DNA/TO=1:1) one may see that there is a partial overlap between absorption/PL and ECD/CPL spectra in the range 500-550 nm. Thus, according to the protocol introduced by Abbate[54,55] observed CPL spectrum should be corrected, since in this range emitted radiation may be re-absorbed (with a preference for *left* or *right* circularly polarized light, according to the ECD spectrum). Indeed, corrected CPL spectrum in the range 550-650 nm is identical with the experimental data, and the difference occurs only in the range between 500-550 nm (Fig. S2).

We may model the situation putting forward that the external binding leaves the TO molecules partly aggregated and exposed to water. In this situation, the TO molecules may preserve a certain degree of internal twist as found by DFT computations for both isolated TO molecules and dimers.[51] All these factors concur in quenching TO fluorescence and consequently in this state the dye would not display any activity in CPL. Nonetheless, a small mole fraction of TO becomes intercalated in DNA even at low mole ratio. This is responsible for the weak but detectable total luminescence and for the positive CPL band. In ECD, it would produce a broad negative signal, which is overwhelmed by the positive couplet due to the external electrostatic binding. On increasing DNA concentration, the dye becomes mostly intercalated into DNA as single molecules. This leads to strong TO fluorescence, which is accompanied by a positive CPL band.

DFT calculations indicated a deep inclusion of TO into ds-DNA,[51] which is compatible with the main and broad negative ECD band observed at high DNA/TO ratios, on assuming that the main electronic transition of this dye is polarized along the major molecular axis.

DNA/DAPI system

To further develop our methodology, we decided to perform an analogous study by using DAPI, which is another fluorescent dye commonly used to stain DNA. DAPI is also intrinsically achiral, but in contrast to TO, it exhibits a strong fluorescence also in water.[48] Furthermore, previous studies revealed that DAPI has complex binding features, which cannot be simply classified, since intercalation, as well as minor and major groove binding modes are possible.[37,56-60]

As before, we initially conducted a complete ECD/absorption titration (Fig. 4), to find the best conditions for CPL measurements. We can make the following observations:

- in the ICD spectrum there is a positive band centred at *ca.* 365 nm;
- although the ICD signal systematically increases on increasing DNA, the shape of ECD band remains constant;
- the absorption spectrum reveals a small redshift of DAPI band upon DNA binding, with an isosbestic point at about 370 nm.

All these features reveal that in the conditions used in this experiment, DAPI is present only in two species: as the free molecule in solution, which is achiral, and as bound to DNA. In this latter case, the sign of the ICD band is positive, which may suggest that DAPI pokes out toward the exterior, as put forward previously,[37] in a very different way compared to TO. Quantitative analysis of the ECD titration through Hildebrand-Benesi method as reported in Ref. [37] leads to an estimate of $\Delta\varepsilon = 31\ M^{-1}\ cm^{-1}$ for DAPI fully bound to DNA, which translates in an Kuhn anisotropy *g*-factor $g_{abs} \approx 1.5 \cdot 10^{-3}$, which is reasonable for an organic dye embedded in the chiral environment provided by DNA.[49]

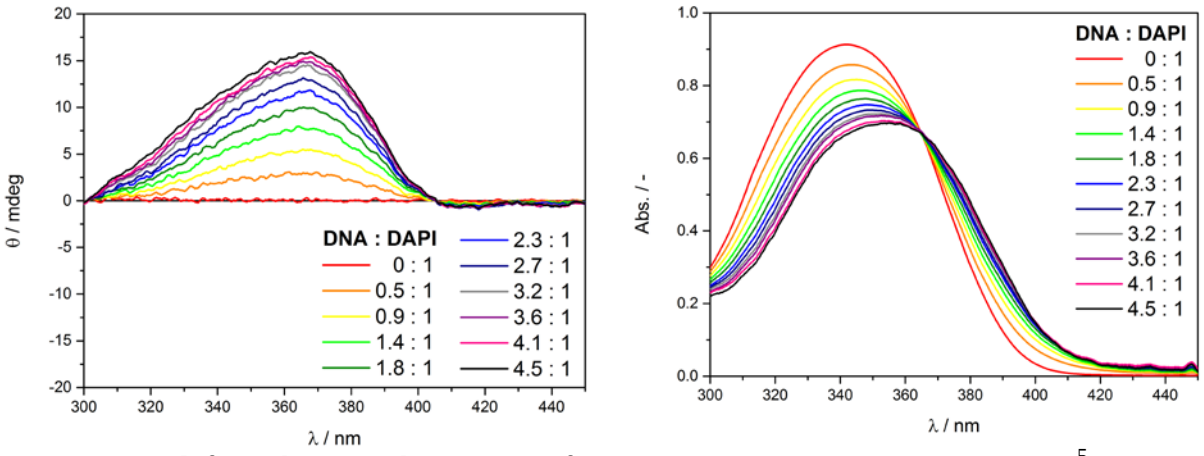

Fig. 4 ECD (left) and UV (right) spectra of DNA/DAPI system ($C_{DAPI} = 3.3 \times 10^{-5}$ M) in 0.1 M NaCl and 0.01 M NaCac buffer (pH = 7.0) measured in 1 cm path length cell.

In the next step of our chiroptical analysis we applied CPL spectroscopy. Since DAPI in water solution is fluorescent by itself, we decided to collect a spectrum without addition of DNA. As it can be seen in Fig. 5, the CPL spectrum in buffer (blue curve) exhibits a broad negative band centred at 475 nm with a high dissymmetry factor $g_{lum} \approx 1 \times 10^{-2}$.

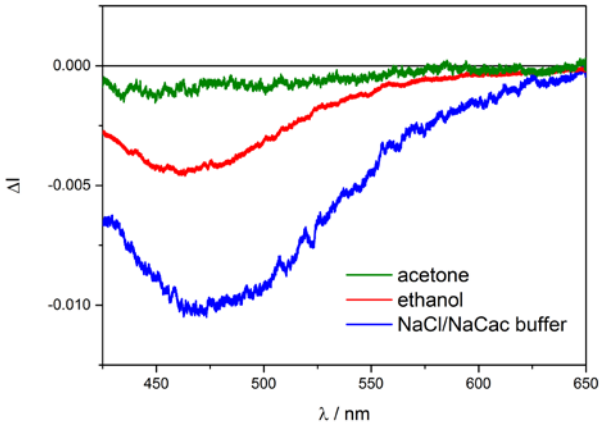

Fig. 5 CPL spectra of DAPI system (C_{DAPI} = 3.3 × 10^{-5} M) in acetone, ethanol and 0.1 M NaCl and 0.01 M NaCac buffer (pH 7.0) measured in the 1 cm path length cell.

This is surely due to an artefact, because DAPI is *achiral*, and to ascertain its origin we conducted additional measurements in different solvents, *i.e.* in ethanol and acetone. It turned out that this effect is significantly reduced in ethanol ($g_{lum} \approx 4 \times 10^{-3}$), while in acetone it is totally absent. These observations demonstrated clearly that the solvent plays a prime role on the onset of these artefacts.

The current configuration of our CPL instrument allows only for 90° excitation/detection geometry, with a consequent danger of photoselecting the luminescent molecules. This phenomenon is well known: if the excitation source is linearly polarized, the molecules whose main transition dipole in absorption is aligned parallel to light polarization are effectively excited, while those with their dipole orthogonal to UV radiation are not. If the subsequent photon emission occurs before the molecules have reoriented, then the exiting light is also linearly polarized (on top of possible circular polarization, which can only stem from chirality). This linear polarization may interfere with the detection optics, originating the artefact.[61]

It is clear that in these conditions our attempts to use CPL for monitoring the interaction of DAPI with DNA would be too error prone and at the moment we decided not to pursue this objective further. Nonetheless, we decided to better understand how such a small molecule as DAPI would give rise to this CPL artefact, on account of its supposedly fast reorientational rate, and consequently understand better the limitations of the presented methodology.

The ^{1}H NMR spectra of DAPI both in D_2O and CD_3OD reveal the expected resonances for this molecule as sharp signals (Figure S3). Apparently, these spectra are compatible with a fast tumbling molecule, with rotational correlation time τ_c well below 1 ns, as also confirmed by measuring the diffusion coefficient, which indicates a hydrodynamic radius of a few Å. This is in apparent conflict with the photoselection process we put forward, because the lifetime of electronic excited state of DAPI amounts to 1.24 ns.[62]

We ran another full set of quantitative ^{1}H NMR experiments by adding directly 1μL of *tert*-BuOH as internal standard to NMR tubes with a known quantity of DAPI dissolved in D_2O and CD_3OD. We found that the integrals of DAPI signals (appropriately scaled for the number of protons) account only for a fraction of the total dye: 15% in water, 76% in methanol. This means that the dye is in slow (NMR timescale) exchange between a fast tumbling free state, responsible for the observed signals and a highly aggregated one, with such a slow reorientation to provide extremely broad and easily saturated NMR signals, which cannot be observed. This condition is met if the τ_c of the aggregates is at least 100 ns or greater. For such that large aggregates, photoselection can be a serious problem. Indeed, from our results in water solution the equilibrium between the free and aggregate form of DAPI is shifted strongly towards the aggregate form, and to a much lesser extent in methanol.

Conclusions

In the present study we have applied chiroptical methods for investigating the binding of TO and DAPI with DNA. In both cases, the analysis of ECD spectra is in good agreement with previous findings. Secondly, for the first time we have applied CPL spectroscopy for studying the interactions between calf thymus DNA and TO as a model fluorescence dye. Although this example is not covering the whole range of dyes used in DNA study, it evidently indicates that CPL can be a useful complement to other measurements for advanced analysis of DNA binding. We believe that our results give a new insight to development of CPL spectroscopy towards sensing DNA and also other bio-compounds. This technique might have some limitations due to photoselection, as it was shown using DAPI, a dye already known to have a complex system of solution equilibria, which may interfere with the measurements and therefore it requires a critical attitude in data collection and interpretation.

Acknowledgements

Financial support from the University of Pisa with grants PRA_2015_38 and PRA_2016_50 is gratefully acknowledged. M.G. thanks the Polish Ministry of Science and Higher Education ('Mobilnosc Plus' grant no. 1286/MOB/IV/2015/0) for the support.

References

[1] E. Fabini, G.M.L. Fiori, D. Tedesco, N.P. Lopes, C. Bertucci, Surface plasmon resonance and circular dichroism characterization of cucurbitacins binding to serum albumins for early pharmacokinetic profiling, J. Pharm. Biomed. Anal. 122 (2016) 166-172.
[2] G. Ascoli, C. Bertucci, P. Salvadori, Stereospecific and competitive-binding of drugs to human serum-albumin - a difference circular-dichroism approach, J. Pharm. Sci. 84(6) (1995) 737-741.
[3] C. Bertucci, G. Ascoli, G. Uccello Barretta, L. Di Bari, P. Salvadori, The binding of 5-fluorouracil to native and modified human serum-albumin - UV, CD, and H-1 and F-19 NMR investigation, J. Pharm. Biomed. Anal. 13(9) (1995) 1087-1093.
[4] C. Bertucci, A. Viegi, G. Ascoli, P. Salvadori, Protein-binding investigation by difference circular-dichroism - native and acetylated human serum albumins, Chirality 7(2) (1995) 57-61.
[5] J.P. Riehl, G. Muller, Circularly polarized luminescence spectroscopy and emission-detected circular dichroism, in: N. Berova, P.L. Polavarapu, K. Nakanishi, R.W. Woody (Eds.), Comprehensive Chiroptical Spectroscopy, John Wiley & Sons, Inc., Hoboken, 2012, pp. 65-90.
[6] F. Zinna, L. Di Bari, Lanthanide circularly polarized luminescence: bases and applications, Chirality 27(1) (2015) 1-13.
[7] R. Carr, N.H. Evans, D. Parker, Lanthanide complexes as chiral probes exploiting circularly polarized luminescence, Chem. Soc. Rev. 41(23) (2012) 7673-7686.
[8] J. Yuasa, T. Ohno, H. Tsumatori, R. Shiba, H. Kamikubo, M. Kataoka, Y. Hasegawa, T. Kawai, Fingerprint signatures of lanthanide circularly polarized luminescence from proteins covalently labeled with a β-diketonate europium(III) chelate, Chem. Commun. 49(41) (2013) 4604-4606.
[9] T.-a. Uchida, K. Nozaki, M. Iwamura, Chiral sensing of various amino acids using induced circularly polarized luminescence from europium(III) complexes of phenanthroline dicarboxylic acid derivatives, Chem. As. J. 11(17) (2016) 2415-2422.

[10] G. Muller, Luminescent chiral lanthanide(III) complexes as potential molecular probes, Dalton Trans. (44) (2009) 9692-9707.
[11] T. Wu, J. Průša, J. Kessler, M. Dračínský, J. Valenta, P. Bouř, Detection of sugars via chirality induced in europium(III) compounds, Anal. Chem. 88(17) (2016) 8878-8885.
[12] S. Orsini, F. Zinna, T. Biver, L. Di Bari, I. Bonaduce, Circularly polarized luminescence reveals interaction between commercial stains and protein matrices used in paintings, RSC Adv. 6(98) (2016) 96176-96181.
[13] S. Pascal, C. Besnard, F. Zinna, L. Di Bari, B. Le Guennic, D. Jacquemin, J. Lacour, Zwitterionic [4]helicene: a water-soluble and reversible pH-triggered ECD/CPL chiroptical switch in the UV and red spectral regions, Org. Biomol. Chem. 14(20) (2016) 4590-4594.
[14] H. Isla, J. Crassous, Helicene-based chiroptical switches, C. R. Chimie 19(1–2) (2016) 39-49.
[15] F. Zinna, U. Giovanella, L. Di Bari, Highly circularly polarized electroluminescence from a chiral europium complex, Adv. Mater. 27(10) (2015) 1791-1795.
[16] J.R. Brandt, X. Wang, Y. Yang, A.J. Campbell, M.J. Fuchter, Circularly polarized phosphorescent electroluminescence with a high dissymmetry factor from PHOLEDs based on a platinahelicene, J. Am. Chem. Soc. 138(31) (2016) 9743-9746.
[17] F. Zinna, M. Pasini, F. Galeotti, C. Botta, L. Di Bari, U. Giovanella, Design of lanthanide-based OLEDs with remarkable circularly polarized electroluminescence, Adv. Funct. Mater. 10.1002/adfm.201603719 (2016).
[18] A. Gafni, Circular dichroism and circular polarization of luminescence of reduced nicotinamide adenine dinucleotide in solution and bound to dehydrogenases, Biochemistry 17(7) (1978) 1301-1304.
[19] G. Bobba, R.S. Dickins, S.D. Kean, C.E. Mathieu, D. Parker, R.D. Peacock, G. Siligardi, M.J. Smith, J.A. Gareth Williams, C.F.G.C. Geraldes, Chiroptical, ESMS and NMR spectroscopic study of the interaction of enantiopure lanthanide complexes with selected self-complementary dodecamer oligonucleotides, J. Chem. Soc. Perkin Trans. 2 (9) (2001) 1729-1737.
[20] S. Abdollahi, W.R. Harris, J.P. Riehl, Application of circularly polarized luminescence spectroscopy to Tb(III) and Eu(III) complexes of transferrins, J. Phys. Chem. 100(5) (1996) 1950-1956.
[21] R. Carr, R. Puckrin, B.K. McMahon, R. Pal, D. Parker, L.O. Pålsson, Induced circularly polarized luminescence arising from anion or protein binding to racemic emissive lanthanide complexes, Methods Appl. Fluoresc. 2(2) (2014).
[22] A. Rybicka, G. Longhi, E. Castiglioni, S. Abbate, W. Dzwolak, V. Babenko, M. Pecul, Thioflavin T: electronic circular dichroism and circularly polarized luminescence induced by amyloid fibrils, ChemPhysChem (2016) 2931-2937.
[23] M. Nakamura, J. Suzuki, F. Ota, T. Takada, K. Akagi, K. Yamana, Helically assembled pyrene arrays on an RNA duplex that exhibit circularly polarized luminescence with excimer formation, Chem. Eur. J. 22(27) (2016) 9121-9124.
[24] J. Hall, T. Renger, F. Müh, R. Picorel, E. Krausz, The lowest-energy chlorophyll of photosystem II is adjacent to the peripheral antenna: Emitting states of CP47 assigned via circularly polarized luminescence, Biochim. Biophys. Acta, Bioenerg. 1857(9) (2016) 1580-1593.
[25] E.E. Gussakovsky, Y. Shahak, H. van Amerongen, V. Barzda, Circularly polarized chlorophyll luminescence reflects the macro-organization of grana in pea chloroplasts, Photosynth. Res. 65(1) (2000) 83-92.
[26] E. Castiglioni, S. Abbate, G. Longhi, Revisiting with updated hardware an old spectroscopic technique: circularly polarized luminescence, App. Spectrosc. 64(12) (2010) 1416-1419.

[27] T. Harada, H. Hayakawa, M. Watanabe, M. Takamoto, A solid-state dedicated circularly polarized luminescence spectrophotometer: Development and application, Rev. Sci. Instrum. 87(7) (2016) 075102.
[28] M. Pecul, K. Ruud, The optical activity of β,γ-enones in ground and excited states using circular dichroism and circularly polarized luminescence, Phys. Chem. Chem. Phys. 13(2) (2011) 643-650.
[29] G. Mazzeo, M. Fuse, G. Longhi, I. Rimoldi, E. Cesarotti, A. Crispini, S. Abbate, Vibrational circular dichroism and chiroptical properties of chiral Ir(III) luminescent complexes, Dalton Trans. 45(3) (2016) 992-999.
[30] F. Zinna, T. Bruhn, C.A. Guido, J. Ahrens, M. Bröring, L. Di Bari, G. Pescitelli, Circularly polarized luminescence from axially chiral BODIPY DYEmers: an experimental and computational study, Chem. Eur. J. 22(45) (2016) 16089-16098.
[31] T. Biver, A. Boggioni, F. Secco, E. Turriani, M. Venturini, S. Yarmoluk, Influence of cyanine dye structure on self-aggregation and interaction with nucleic acids: A kinetic approach to TO and BO binding, Arch. Biochem. Biophys. 465(1) (2007) 90-100.
[32] M. Tanaka, N. Shigi, J. Sumaoka, M. Komiyama, Thiazole orange-conjugated peptide nucleic acid for fluorescent detection of specific DNA sequences and site-selective photodamage, RSC Adv. 4(108) (2014) 63533-63538.
[33] Y.-P. Xing, C. Liu, X.-H. Zhou, H.-C. Shi, Label-free detection of kanamycin based on a G-quadruplex DNA aptamer-based fluorescent intercalator displacement assay, Scientific Reports 5 (2015) 8125.
[34] N. Polley, P.K. Sarkar, S. Chakrabarti, P. Lemmens, S.K. Pal, DNA Biomaterial Based Fiber Optic Sensor: Characterization and Application for Monitoring in situ Mercury Pollution, ChemistrySelect 1(11) (2016) 2916-2922.
[35] S. Choudhury, B. Ghosh, P. Singh, R. Ghosh, S. Roy, S.K. Pal, Ultrafast differential flexibility of Cro-protein binding domains of two operator DNAs with different sequences, Phys. Chem. Chem. Phys. 18(27) (2016) 17983-17990.
[36] T. Biver, D. Lombardi, F. Secco, M. Rosaria Tine, M. Venturini, A. Bencini, A. Bianchi, B. Valtancoli, Kinetic and equilibrium studies on the polyazamacrocycle neotetren: metal-complex formation and DNA interaction, Dalton Trans. (12) (2006) 1524-1533.
[37] M.R. Beccia, T. Biver, A. Pardini, J. Spinelli, F. Secco, M. Venturini, N. Busto Vázquez, M.P. Lopez Cornejo, V.I. Martin Herrera, R. Prado Gotor, The fluorophore 4',6-diamidino-2-phenylindole (DAPI) induces DNA folding in long double-stranded DNA, Chem. As. J. 7(8) (2012) 1803-1810.
[38] D. Monchaud, C. Allain, M.P. Teulade-Fichou, Thiazole Orange: a useful probe for fluorescence sensing of G-quadruplex–ligand Interactions, Nucleos. Nucleot. Nucl. 26(10-12) (2007) 1585-1588.
[39] J. Ghasemi, S. Ahmadi, A.I. Ahmad, S. Ghobadi, Spectroscopic characterization of Thiazole Orange-3 DNA interaction, Appl. Biochem. Biotechnol. 149(1) (2008) 9-22.
[40] D.V. Jarikote, N. Krebs, S. Tannert, B. Röder, O. Seitz, Exploring base-pair-specific optical properties of the DNA stain Thiazole Orange, Chem. Eur. J. 13(1) (2007) 300-310.
[41] S. Nakayama, I. Kelsey, J. Wang, K. Roelofs, B. Stefane, Y. Luo, V.T. Lee, H.O. Sintim, Thiazole Orange-induced c-di-GMP quadruplex formation facilitates a simple fluorescent detection of this ubiquitous biofilm regulating molecule, J. Am. Chem. Soc. 133(13) (2011) 4856-4864.
[42] S. Berndl, S.D. Dimitrov, F. Menacher, T. Fiebig, H.-A. Wagenknecht, Thiazole Orange dimers in DNA: fluorescent base substitutions with hybridization readout, Chem. Eur. J. 22(7) (2016) 2386-2395.
[43] I. Lubitz, D. Zikich, A. Kotlyar, Specific high-affinity binding of Thiazole Orange to triplex and G-quadruplex DNA, Biochemistry 49(17) (2010) 3567-3574.

[44] C.C. Trevithick-Sutton, L. Mikelsons, V. Filippenko, J.C. Scaiano, Effect of UVC-induced damage to DNA on the Intercalation of Thiazole Orange: a convenient reporter for DNA Damage, Photochem. Photobiol. 83(3) (2007) 556-562.
[45] P. Guo, A. Paul, A. Kumar, A.A. Farahat, D. Kumar, S. Wang, D.W. Boykin, W.D. Wilson, The thiophene "Sigma-Hole" as a concept for preorganized, specific recognition of G-C base pairs in the DNA minor groove, Chem. Eur. J. 22(43) (2016) 15404-15412.
[46] D. Tedesco, C. Bertucci, Induced circular dichroism as a tool to investigate the binding of drugs to carrier proteins: Classic approaches and new trends, J. Pharm. Biomed. Anal. 113 (2015) 34-42.
[47] T. Biver, Use of UV-vis spectrometry to gain information on the mode of binding of small molecules to DNAs and RNAs, Appl. Spectrosc. Rev. 47(4) (2012) 272-325.
[48] G. Pescitelli, L. Di Bari, N. Berova, Application of electronic circular dichroism in the study of supramolecular systems, Chem. Soc. Rev. 43 (2014) 5211-5233.
[49] N. Berova, L. Di Bari, G. Pescitelli, Application of electronic circular dichroism in configurational and conformational analysis of organic compounds, Chem. Soc. Rev. 36(6) (2007) 914-931.
[50] In the previously published work, the overall intensity of the Absorption spectra are somewhat different from the ones found here, although the quantitative analysis through Hildebrand-Benesi method leads to very similar results. It is possible that this different behaviour stems from the different degree of DNA fragmentation.
[51] A. Biancardi, T. Biver, A. Marini, B. Mennucci, F. Secco, Thiazole orange (TO) as a light-switch probe: a combined quantum-mechanical and spectroscopic study, Phys. Chem. Chem. Phys. 13 (2011) 12595-12602.
[52] T.Y. Ogul'chansky, M.Y. Losytskyy, V.B. Kovalska, V.M. Yashchuk, S.M. Yarmoluk, Interaction of cyanine dyes with nucleic acids. XXIV. Aggregation of monomethine cyanine dyes in presence of DNA and its manifestation in absorption and fluorescence spectra, Spectrochim. Acta A 57 (2001) 1525-1532.
[53] P.E. Schipper, B. Nordén, F. Tjerneld, Determination of binding geometry of DNA-adduct systems through induced circular dichroism, Chem. Phys. Lett. 70(1) (1980) 17-21.
[54] E. Castiglioni, S. Abbate, F. Lebon, G. Longhi, Ultraviolet, Circular Dichroism, Fluorescence, and Circularly Polarized Luminescence Spectra of Regioregular Poly-[3-((S)-2-Methylbutyl)-Thiophene] in Solution, Chirality 24(9) (2012) 725-730.
[55] G. Longhi, E. Castiglioni, J. Koshoubu, G. Mazzeo, S. Abbate, Circularly Polarized Luminescence: A Review of Experimental and Theoretical Aspects, Chirality 28(10) (2016) 696-707.
[56] A. Biancardi, T. Biver, F. Secco, B. Mennucci, An investigation of the photophysical properties of minor groove bound and intercalated DAPI through quantum-mechanical and spectroscopic tools, Phys. Chem. Chem. Phys. 15(13) (2013) 4596-4603.
[57] F.A. Tanious, J.M. Veal, H. Buczak, L.S. Ratmeyer, W.D. Wilson, DAPI (4',6-diamidino-2-phenylindole) binds differently to DNA and RNA: minor-groove binding at AT sites and intercalation at AU sites, Biochemistry 31(12) (1992) 3103-3112.
[58] S. Eriksson, S.K. Kim, M. Kubista, B. Norden, Binding of 4',6-diamidino-2-phenylindole (DAPI) to AT regions of DNA: Evidence for an allosteric conformational change, Biochemistry 32(12) (1993) 2987-2998.
[59] J. Kapuscinski, DAPI: a DNA-specific fluorescent probe, Biotech. Histochem. 70(5) (1995) 220-233.
[60] Y. Kubota, K. Kubota, S. Tani, DNA binding properties of DAPI (4′,6-diamidino-2-phenylindole) analogs having an imidazoline ring or a tetrahydropyrimidine ring: Groove-binding and intercalation, Nucleic Acids Symp. Ser. 44(1) (2000) 53-54.

[61] H.P.J.M. Dekkers, P.F. Moraal, J.M. Timper, J.P. Riehl, Optical Artifacts in Circularly Polarized Luminescence Spectroscopy, Appl. Spectrosc. 39 (1985) 818-821.
[62] J.R. Lakowicz, Principles of Fluorescence Spectroscopy, 3rd ed., Springer, 2006.